ELSEVIER

Selective glucocorticoid receptor nonsteroidal ligands completely antagonize the dexamethasone mediated induction of enzymes involved in gluconeogenesis and glutamine metabolism

Monica Einstein[a,*], Mark Greenlee[b], Greg Rouen[b], Ayesha Sitlani[a], Joe Santoro[a], Chuanlin Wang[a], Shilpa Pandit[a], Paul Mazur[a], Isabella Smalera[a], Alehna PM Weaver[a], Ying Ying Zeng[c], Lan Ge[a], Theresa Kelly[a], Tony Paiva[a], Wayne Geissler[a], Ralph T. Mosley[c], Joanne Williamson[a], Amjad Ali[b], Jim Balkovec[b], Georgianna Harris[a]

[a] *Department of Metabolic Disorders, Merck Research Laboratories, P.O. Box 2000, Mail Code: RY80N-C31, Rahway, NJ 07065, USA*
[b] *Department of Medicinal Chemistry, Merck Research Laboratories, Rahway, NJ, USA*
[c] *Department of Molecular Modelling, Merck Research Laboratories, Rahway, NJ, USA*

Abstract

Glucocorticoids (GCs) are vital multi-faceted hormones with recognized effects on carbohydrate, protein and lipid metabolism. Previous studies with the steroid antagonist, RU486 have underscored the essential role of GCs in the regulation of these metabolic pathways. This article describes the discovery and characterization of novel GRα selective nonsteroidal antagonists (NSGCAs). NSGCAs **2** and **3** are spirocyclic dihydropyridine derivatives that selectively bind the GRα with IC_{50s} of 2 and 1.5 nM, respectively. Importantly, these compounds are full antagonists of the induction by dexamethasone (Dex) of marker genes for glucose and glutamine metabolism; the tyrosine amino transferase (TAT) and glutamine synthetase (GS) enzymes, respectively. In contrast, GC-dependent transcriptional repression of the collagenase 1 (MMP-1) enzyme, an established GRα responsive proinflammatory gene; is poorly antagonized by these compounds. These NSGCAs might have useful applications as tools in metabolic research and drug discovery.
© 2004 Elsevier Ltd. All rights reserved.

Keywords: Glucocorticoid; Dexamethasone; NSGCA

1. Introduction

Glucocorticoids (GCs) are essential for a diversified spectrum of physiological functions, including tissue differentiation, carbohydrate, protein and lipid metabolism as well as its recognized anti-inflammatory actions. It is well established that (GC) effects are primarily mediated by a ligand-dependent transcriptional mechanism through the glucocorticoid receptor (GRα). Depending on the structure of the promoter and the composition of other transcriptional regulatory proteins that are bound to the target promoter; activation of the GR can result in either the potentiation or repression of the transcription rate of target genes by distinct mechanisms. For example, GCs repress the transcription rate of proinflammatory genes such as AP-1 and NF-KB largely by a protein–protein interaction mechanism between the GR and these transcription factors. By contrast, GR transactivation is mediated through the binding of GRα homodimers to so-called glucocorticoid response elements (GREs) in the upstream regions of GC target promoters. The phosphoenolpyruvate carboxykinase (PEPCK), tyrosine amino-

* Corresponding author.
E-mail address: monica_einstein@merck.com (M. Einstein).

transferase (TAT) and the glutamine synthetase (GS) genes are three well characterized GRα metabolic target genes; [11,12,19] that are induced by natural and synthetic GCs via a GRE mediated mechanism.

In recent years, the GR/progesterone receptor (PR) antagonist, RU486 has been an invaluable tool in demonstrating the essential role of GCs in the induction of gluconeogenic enzymes, in vitro and in vivo. Notably, in the db/db animal model of insulin resistance, treatment of these animals with RU486 led to significant reductions in the mRNA levels of gluconeogenic enzymes such as, TAT, PEPCK, glucose-6-phosphatase, and the Glut-2 transporter; with a concomitant 49% reduction in the plasma blood glucose levels; [7,8] underscoring a causal relationship between GC induction of gluconeogenic enzymes and the onset of hyperglycemia. Moreover, in the diet-induced high-fat-fed (DIO) rodent model, RU486 improved the insulin resistance caused by high fat feeding in skeletal muscles by 62–68% [16]. Finally, in man, treatment of healthy human males with RU486 was shown to reverse the acute catabolic effects of hypercortisolemia on glucose and leucine metabolism [9]. Thus, based on this extensive, compelling literature on the anti-diabetic actions of RU486 in various animal models of insulin resistance and man, we reasoned that a GRα antagonist is a viable approach to lowering plasma glucose levels.

In this paper, we describe the discovery and characterization of novel and potent nonsteroidal (NSGCAs) ligands of GRα. These compounds are selective for GRα with greatly reduced binding to the androgen receptor (AR), mineralocorticoid receptor (MR) and PR. In functional assays in cells, these NSGCAs completely antagonized the GRE-mediated dependent induction by Dex of both endogenous and reporter-based promoters. In contrast, these compounds are weak antagonists of the Dex dependent repression of a pro-inflammatory gene, MMP-1.

To our knowledge this is the first description of spirocyclic dihydropyridine NSGCAs that antagonize transcriptional readouts of glucose and glutamine metabolism with attenuated effects on the anti-inflammatory activity of the endogenous GRα in the A549 cell line. The implications and the potential therapeutic utility of these novel GRα selective NSGCAs are also discussed.

2. Material and methods

2.1. Reagents

[1,2,4,6,7-^{3}H] Dex with a specific activity (~84 Ci/mmol) was purchased from Amersham Biotechnologies and was utilized for all the ligand binding studies. Non-radioactive Dex, progesterone, aldosterone was purchased from Sigma. Cell culture reagents were purchased from LIFE Technologies. ^{3}H-progesterone and ^{3}H-aldosterone were purchased from NEN.

2.2. Synthesis of compounds

2.2.1. 1-(1,3-Indanedion-2-ylidene)-2-acenaphthenone (10) [24]

A mixture of 1,3-indandione (9.73 g, 66.58 mmol), glacial acetic acid (45 ml), and conc. HCl (2.3 ml) was added to a stirring room temperature mixture of acenaphthenequinone (6.82 g, 37.44 mmol) in glacial acetic acid (230 ml). The reaction vessel was fitted with a reflux condenser and the mixture was heated at 100 °C for 3 h. The resulting dark green solution was removed from the heating source and allowed to stand overnight. The precipitate formed overnight was collected by filtration, washed with cold methanol, and dried in a vacuum desiccator to afford 9.3 g (55% yield) of a crude gray-green powder.

A portion of this solid (1.61 g, 3.53 mmol) was treated with conc. H$_2$SO$_4$ (16 ml) and the thick, dark green solution was stirred at room temperature for 20 min. This mixture was carefully poured into an Erlenmeyer containing 150 ml of rapidly stirring room temperature H$_2$O and the resulting red precipitate was stirred for an additional 20 min. Solids were collected by suction filtration and the red filter cake was washed thoroughly with hot H$_2$O (4 × 300 ml, 80 °C), and dried in a vacuum desiccator. The crude solid was purified by flash chromatography on silica gel (3–5% ethyl acetate/methylene chloride), followed by recrystallization from chloroform/hexane (1:2) to give 10 as a bright red crystalline solid (661 mg, 60% yield). ^{1}H NMR (CDCl$_3$) δ 7.78–7.89 (m, 4H), 8.04–8.17 (m, 4H), 9.56 (d, J = 7.5 Hz, 2H); MS (ESI) m/z: 311.0 (M + 1).

2.2.2. 2,5′-Dioxo-2′-methyl-3′-N-phenylcarbamoyl-spiro{1,4′-acenaphthene-1′,4′-dihydroindeno [3,2-b]pyridine} (1)

Preparation of 11a (R^1 = CONHPh, R^2 = Me): acetoacetanilide (1.76 g, 9.93 mmol) and ammonium acetate (1.15 g, 14.9 mmol) were mixed in 16.5 ml of absolute ethanol and refluxed at 80 °C for 24 h glucocorticoids (GCs). The solvent was removed under reduced pressure to give 11a as a waxy yellow solid (~75% pure) which was used crude in the following reaction.

To a stirring, room temperature solution of 10 (168.7 mg, 0.547 mmol) in glacial acetic acid (15 ml) under an atmosphere of N$_2$ was added crude 11a (815 mg). The reaction vessel was fitted with a reflux condenser and the mixture was heated at 100 °C for 5 h. The resulting dark red solution was removed from the heating source and allowed to stand at room temperature until a precipitate formed (24–48 h). The red precipitate was isolated by centrifugation and purified by sonication with glacial acetic acid and re-isolation by centrifugation. Drying in a vacuum desiccator gave 1 as a fine red solid (111.9 mg, 45% yield). ^{1}H NMR (DMSO) δ 2.54 (s, 3H), 6.85 (d, J = 6.6 Hz, 1H), 6.97 (d, J = 8.0 Hz, 2H), 7.08 (d, J = 7.2 Hz, 1H), 7.19–7.32 (m, 6H), 7.45 (t, J = 7.4 Hz, 2H), 7.68 (t, J = 7.9 Hz, 3H), 10.47 (s, 1H), 11.69 (s, 1H); MS (ESI) m/z: 469.2 (M + 1).

2.2.3. 2,5′-Dioxo-2′-methyl-3′-ethoxycarbonyl-spiro{1,4′-acenaphthene-1′,4′-dihydroindeno[3,2-b]pyridine} (2)

Compound **2** was prepared from **10** (86.0 mg, 0.277 mmol) and commercially available (Aldrich) ethyl-3-aminocrotonate **11b** ($R^1 = CO_2Et$, $R^2 = Me$; 220 µl, 1.75 mmol) in a similar manner to the preparation of **1**. The bright red solid (87.4 mg) was obtained in 75% yield. ^{1}H NMR (DMSO) δ 0.10 (t, $J = 7.1$ Hz, 3H), 2.48 (s, 3H), 3.38 (m, 2H), 7.04 (d, $J = 7.1$ Hz, 1H), 7.29 (d, $J = 7.6$ Hz, 1H), 7.33 (d, $J = 7.1$ Hz, 1H), 7.45 (t, $J = 7.1$ Hz, 1H), 7.56 (t, $J = 7.6$ Hz, 1H), 7.66 (d, $J = 7.3$ Hz, 1H), 7.80 (t, $J = 7.6$ Hz, 1H), 7.85 (d, $J = 8.3$ Hz, 1H), 7.88 (d, $J = 6.8$ Hz, 1H), 8.19 (d, $J = 8.1$ Hz, 1H), 10.47 (s, 1H); MS (ESI) m/z: 422.2 ($M + 1$).

2.2.4. 2,5′-Dioxo-2′-methyl-3′-benzyloxycarbonyl-spiro{1,4′-acenaphthene-1′,4′-dihydroindeno[3,2-b]pyridine} (3)

Preparation of **11c** ($R^1 = CO_2Bn$, $R^2 = Me$): reagent grade NH_4OH (0.81 ml, 12.02 mmol) was added dropwise to a stirring, room temperature slurry of benzyl acetoacetate (1.73 ml, 10.01 mmol), absolute ethanol (14 ml), and montmorillonite K-10 (3 g) [5]. The mixture was stirred at r.t. overnight and then filtered, washing the filter cake with ethanol. The solvent was removed in vacuo and purification was performed by flash chromatography on silica gel (30% ethyl acetate/hexanes) to afford **11c** as a pale yellow oil (1.28 g, 67% yield).

Compound **3** was prepared from **10** (114.0 mg, 0.367 mmol) and **11c** (398 µl, 2.31 mmol) in a similar manner to the preparation of **1**. The red solid (124.0 mg) was obtained in 70% yield. ^{1}H NMR (DMSO) δ 2.49 (s, 3H), 4.44 (d, $J = 12.6$ Hz, 1H), 4.52 (d, $J = 12.6$ Hz, 1H), 6.51 (d, $J = 7.3$ Hz, 2H), 7.03 (d, $J = 7.1$ Hz, 1H), 7.07 (dd, $J = 7.4$ Hz and $J = 7.3$ Hz, 2H), 7.14 (t, $J = 7.4$ Hz, 1H), 7.29 (t, $J = 7.4$ Hz, 1H), 7.33 (d, $J = 6.9$ Hz, 1H), 7.45 (t, $J = 7.5$ Hz, 1H), 7.54 (t, $J = 6.9$ Hz, 1H), 7.66 (d, $J = 7.4$ Hz, 1H), 7.70 (t, $J = 7.6$ Hz, 1H), 7.76 (d, $J = 6.8$ Hz, 1H), 7.84 (d, $J = 8.3$ Hz, 1H), 8.12 (d, $J = 8.1$ Hz, 1H), 10.49 (s, 1H); ^{13}C NMR (DMSO) 20.04, 54.65, 65.74, 106.33, 108.97, 120.38, 120.79, 121.18, 121.38, 124.92, 127.92, 128.00, 128.19, 128.70, 128.91, 129.24, 130.15, 131.14, 132.71, 133.36, 134.26, 135.89, 136.24, 140.88, 145.63, 148.20, 154.14, 166.26, 190.14, 205.41 ppm; MS (ESI) m/z: 484.2 ($M + 1$).

2.2.5. 2,5′-Dioxo-2′-methyl-3′-N-benzylcarbamoyl-spiro{1,4′-acenaphthene-1′,4′-dihydroindeno[3,2-b]pyridine} (4)

Preparation of **11d** ($R^1 = CONHBn$, $R^2 = Me$): N-benzyl-3-oxobutanamide (956.9 mg, 5.00 mmol) and ammonium acetate (578.6 mg, 7.50 mmol) were mixed in 8.5 ml of absolute ethanol and refluxed at 80 °C for 24 h. The solvent was removed under reduced pressure to give **11d** as a waxy yellow solid (∼75% pure) which was used crude in the following reaction.

Compound **4** was prepared from **10** (246.8 mg, 0.795 mmol) and crude **11d** (1.27 g) in a similar manner to the preparation of **1**, with the exception that a precipitate did not spontaneously form upon prolonged standing at room temperature. Instead, the crude reaction mixture was partitioned between ethyl acetate and water. The organic layer was washed with water and brine, dried (Na_2SO_4), filtered and evaporated in vacuo. The crude oil was purified by flash chromatography on silica gel (5% methanol/methylene chloride) to give 238 mg of **4** as an orange oil (62% yield). ^{1}H NMR (DMSO) δ 2.52 (s, 3H), 4.45 (d, $J = 16.0$ Hz, 1H), 4.52 (d, $J = 16$ Hz, 1H), 6.51 (s, 1H), 6.58 (d, $J = 7.4$ Hz, 2H), 6.90–6.97 (m, 4H), 7.07 (d, $J = 7.1$ Hz, 1H), 7.17 (d, $J = 6.9$ Hz, 1H), 7.30 (t, $J = 7.4$ Hz, 1H), 7.39 (t, $J = 7.3$ Hz, 1H), 7.42–7.47 (m, 2H), 7.58 (d, $J = 6.8$ Hz, 1H), 7.67–7.71 (m, 2H), 10.59 (s, 1H); MS (ESI) m/z: 483.2 ($M + 1$).

2.2.6. 2,5′-Dioxo-2′-methyl-3′-N,N-diethylcarbamoyl-spiro{1,4′-acenaphthene-1′,4′-dihydroindeno[3,2-b]pyridine} (5)

Preparation of **11e** ($R^1 = CONEt_2$, $R^2 = Me$): N,N-diethylacetoacetamide (1.63 ml, 10.30 mmol) and ammonium acetate (1.16 g, 15.05 mmol) were mixed in 16.5 ml of absolute ethanol and refluxed at 80 °C for 24 h. The solvent was removed under reduced pressure to give **11e** as a hazy yellow oil (∼75% pure) which was used crude in the following reaction.

Compound **5** was prepared from **10** (249.1 mg, 0.803 mmol) and **11e** (0.48 ml) in a similar manner to the preparation of **1**, with the exception that addition of seed crystals was necessary to induce precipitation [seed crystals were produced by dropwise addition of a small amount of crude reaction mixture (∼0.5 ml) to a stirring, r.t. solution of EtOAc or Et_2O (∼1 ml)]. The red solid (109.1 mg) was obtained in 30% yield. ^{1}H NMR (DMSO) δ 0.06 (t, $J = 6.9$ Hz, 3H), 0.84 (t, $J = 6.9$ Hz, 3H), 1.95 (s, 3H), 2.60–2.65 (m, 1H), 2.83–2.96 (m, 1H), 2.97–3.03 (m, 1H), 3.35–3.42 (m, 1H), 7.08 (d, $J = 7.1$ Hz, 1H), 7.32 (t, $J = 7.4$ Hz, 1H), 7.43 (d, $J = 6.7$ Hz, 1H), 7.46 (d, $J = 7.1$ Hz, 1H), 7.57 (t, $J = 6.9$ Hz, 1H), 7.64 (d, $J = 7.4$ Hz, 1H), 7.75 (t, $J = 7.6$ Hz, 1H), 7.82 (d, $J = 6.8$, 1H), 7.87 (d, $J = 8.5$ Hz, 1H), 8.14 (d, $J = 8.0$ Hz, 1H), 10.20 (s, 1H); MS (ESI) m/z: 449.2 ($M + 1$).

2.2.7. 2,5′-Dioxo-2′-phenyl-3′-ethoxycarbonyl-spiro{1,4′-acenaphthene-1′,4′-dihydroindeno[3,2-b]pyridine} (6)

Preparation of **11f** ($R^1 = CO_2Et$, $R^2 = Ph$) [17]: ethyl benzoylacetate (1.79 ml, 10.34 mmol) and ammonium acetate (1.16 g, 15.05 mmol) were mixed in 16.5 ml of absolute ethanol and refluxed at 80 °C for 24 h. The solvent was removed under reduced pressure, and the residue was flash chromatographed on silica gel (20% ethyl acetate/hexanes) to give **11f** as a yellow oil (1.77 g) in 90% yield.

Compound **6** was prepared from **10** (305.8 mg, 0.985 mmol) and **11f** (1.1 ml, 6.21 mmol) in a similar manner to the preparation of **1**. The bright red solid (270.8 mg)

was obtained in 57% yield. ^{1}H NMR (DMSO) δ 0.10 (t, $J = 7.1$ Hz, 3H), 3.20 (m, 2H), 7.07 (d, $J = 7.1$ Hz, 1H), 7.30 (t, $J = 7.4$ Hz, 1H), 7.41 (t, $J = 7.6$ Hz, 1H), 7.44–7.51 (m, 6H), 7.61 (t, $J = 7.7$ Hz, 1H), 7.76 (d, $J = 7.3$ Hz, 1H), 7.81 (t, $J = 7.6$ Hz, 1H), 7.89 (d, $J = 8.4$ Hz, 1H), 7.92 (d, $J = 6.9$ Hz, 1H), 8.21 (d, $J = 8.0$ Hz, 1H), 10.76 (s, 1H); MS (ESI) m/z: 484.2 ($M + 1$).

2.2.8. 2,5′-Dioxo-1′,2′-dimethyl-3′-ethoxycarbonyl-spiro{1,4′-acenaphthene-1′,4′-dihydroindeno[3,2-b]pyridine} (7)

To a stirred solution of **2** (22.3 mg, 0.053 mmol) in anhydrous DMF (1.0 ml), was added a suspension of freshly washed sodium hydride (60% dispersion, 6.4 mg, 0.159 mmol) in DMF (0.5 ml) at room temperature under an atmosphere of N$_2$. After 10 min, methyl iodide (0.02 ml, 0.321 mmol) was slowly added, and the dark red solution was stirred at 25 °C for 1 h. The reaction mixture was diluted into ethyl acetate and the organic layer was washed with water and brine, dried (Na$_2$SO$_4$), filtered and evaporated in vacuo. The crude red oil was chromatographed by preparative TLC on silica gel (50% ethyl acetate/hexanes) to give **7** as a crunchy red foam (15.6 mg) in 68% yield. ^{1}H NMR (CDCl$_3$) δ 0.11 (t, $J = 7.1$ Hz, 3H), 2.55 (s, 3H), 3.47 (m, 2H), 3.73 (s, 3H), 7.16–7.20 (m, 2H), 7.27 (t, $J = 6.7$ Hz, 1H), 7.35 (d, $J = 6.6$ Hz, 1H), 7.41 (d, $J = 7.5$ Hz, 1H), 7.54 (t, $J = 7.7$ Hz, 1H), 7.75 (t, $J = 7.6$ Hz, 1H), 7.80 (d, $J = 8.2$ Hz, 1H), 8.03 (d, $J = 7.1$ Hz, 1H), 8.09 (d, $J = 8.0$ Hz, 1H); ^{13}C NMR (CDCl$_3$) 12.57, 17.29, 36.11, 54.61, 60.29, 110.41, 111.29, 120.44, 121.73, 121.88, 122.01, 124.72, 128.44, 128.73, 130.10, 130.22, 130.97, 131.87, 134.09, 134.21, 137.23, 141.62, 144.42, 148.60, 157.30, 166.83, 190.20, 205.53; MS (ESI) m/z: 436.2 ($M + 1$).

2.2.9. 2,5′-Dioxo-1′-benzyl-2′-methyl-3′-ethoxycarbonyl-spiro{1,4′-acenaphthene-1′,4′-dihydroindeno[3,2-b]pyridine} (8)

Compound **8** was prepared from **2** (20.2 mg, 0.048 mmol), sodium hydride (60% dispersion, 4.0 mg, 0.098 mmol), benzyl bromide (21.0 µl, 0.177 mmol), and anhydrous DMF (1.4 ml) in a similar manner to the preparation of **7**. The crude red oil was chromatographed by preparative TLC on silica gel (3% methanol/methylene chloride) to give **8** as a dark red oil (14.0 mg) in 57% yield. ^{1}H NMR (CDCl$_3$) δ 0.11 (t, $J = 7.2$ Hz, 3H), 2.45 (s, 3H), 3.46 (m, 2H), 5.38 (s, 2H), 7.01 (d, $J = 7.5$, 1H), 7.09 (t, $J = 7.3$ Hz, 1H), 7.12–7.17 (m, 2H), 7.28–7.42 (m, 2H), 7.45 (d, $J = 7.3$ Hz, 2H), 7.50 (t, $J = 7.7$ Hz, 2H), 7.58 (t, $J = 7.7$ Hz, 1H), 7.78 (t, $J = 7.6$ Hz, 1H), 7.83 (d, $J = 8.2$ Hz, 1H), 8.07 (d, $J = 6.8$ Hz, 1H), 8.11 (d, $J = 8.3$ Hz, 1H); ^{13}C NMR (CDCl$_3$) 12.55, 16.63, 51.19, 60.35, 110.96, 111.57, 115.25, 120.57, 121.75, 121.86, 124.82, 125.82, 127.99, 128.29, 128.49, 128.73, 129.73, 130.01, 130.13, 131.01, 132.03, 134.03, 135.42, 136.75, 137.10, 141.84, 144.34, 148.10, 157.21, 166.86, 190.35, 205.35; MS (ESI) m/z: 512.2 ($M + 1$).

2.2.10. 2,5′-Dioxo-1′-(ethoxymethyl)-2′-methyl-3′-ethoxycarbonyl-spiro{1,4′-acenaphthene-1′,4′-dihydroindeno[3,2-b]pyridine} (9)

Compound **9** was prepared from **2** (233.7 mg, 0.555 mmol), sodium hydride (60% dispersion, 33.3 mg, 0.832 mmol), chloromethyl ethyl ether (103.0 µl, 1.11 mmol), and anhydrous DMF (15.8 ml) in a similar manner to the preparation of **7**. The crude red oil was purified by flash chromatography on silica gel (10% ethyl acetate/methylene chloride) to give **9** as a fine red solid (155.7 mg) in 59% yield. ^{1}H NMR (CDCl$_3$) δ 0.10 (t, $J = 7.1$ Hz, 3H), 1.42 (t, $J = 7.1$ Hz, 3H) 2.63 (s, 3H), 3.45 (m, 2H), 3.78 (m, 2H), 5.26 (d, $J = 10.5$ Hz, 1H), 5.33 (d, $J = 10.5$, 1H), 7.18 (d, $J = 6.9$ Hz, 1H), 7.22 (t, $J = 7.1$ Hz, 1H), 7.31–7.37 (m, 3H), 7.55 (t, $J = 8.0$ Hz, 1H), 7.76 (t, $J = 7.9$ Hz, 1H), 7.81 (d, $J = 8.5$ Hz, 1H), 8.03 (d, $J = 7.1$ Hz, 1H), 8.10 (d, $J = 8.2$ Hz, 1H); MS (ESI) m/z: 434.2 (M–OEt).

2.3. Constructs

The reporter expression vector pMAMNeo-luciferase containing the MMTV LTR upstream of the gene encoding luciferase was purchased from Clontech and was utilized to stably integrate this plasmid into the A549 cell line according to the manufacturer's instructions (LIFE Technologies). The baculovirus expression vector pFASBac (LIFE Technologies) containing the full length human glucocorticoid receptor (hGRα) was made by subcloning the hGRα from the expression vector pKRC2 that was purchased from ATCC. The full length rat MR was amplified by the PCR from a rat kidney cDNA library using the following oligonucleotides: 5′-GTCGACATGGAAACCAAAGGCT-ACCACAGTCTCC3-′ (MR sense) and 5′-GGTACCTCA-CTTTCTGTGAAAGTAAAGGGGTTTGGC-3′ (MR antisense). The sequence was confirmed and the rat MR clone was subcloned into the pFASBac baculovirus expression vector for expression.

2.4. Ligand binding assays

For hGRα and rMR ligand binding assays cytosols were prepared from recombinant baculovirus expressed receptors. For hPR binding assays, hPR cytosols were made from the T-47D cell line. For all the receptors tested, frozen cell pellets were dounce homogenized in ice cold KPO$_4$ buffer (10 mM KPO$_4$, 20 mM sodium molybdate, 1 mM EDTA, 5 mM DTT and complete protease inhibitor tablets from Boehringer Mannheim) with a "B" plunger. The homogenates were centrifuged at 35,000 × g for 1 h at 4 °C in a JA-20 rotor. For GRα, the IC$_{50s}$ were determined by incubating the cytosols at a final concentration of 2.5 nM [1,2,4,6,7-^{3}H] Dex in the presence of full log scale concentrations (10^{-11} to 10^{-6}) of cold Dex or the ligands at 4 °C for 24 h. Bound and free were separated by a gel filtration assay. The reaction plate was centrifuged at 1000 × g for 5 min and the flow thru was collected in a second 96-well plate. Scintillation cocktail was added and

counted in a double coincidence beta counter (Wallac). Assays for MR and PR were performed in a similar fashion with 2 nM [³H]-aldosterone and 5 nM [³H]-progesterone, respectively. For whole cell ligand binding assay, 200,000 cells/well for the A549, hSKM cells, L6 or H4IIE were seeded on a 24-well plate in the media described below for these cell lines. The cells were incubated with at a final concentration of 10 nM [1,2,4,6,7-³H] Dex (~84 Ci/mmol) in the presence of increasing concentrations (10^{-11} to 10^{-6}) of cold Dex or the ligands at 37 °C for 2 h. The cells were then washed 2× with 1× PBS (Ca^{2+}, Mg^{2+} free) (LIFE Technologies). Scintillation fluid was added to the cell extracts and the plates were counted in the beta scintillation counter (Wallac). The IC_{50}s for both the in vitro and whole cell binding assays were calculated with the GraphPad Prism 3.0 software package using a single binding site sigmoidal dose response model. The data reported is derived from the duplicate wells from three independent experiments.

2.5. Cell culture, cell-based assays with endogenous and reporter-based promoters

The human lung epithelial cell line A549, the rat hepatoma cell line H4-IIE, the L6 rat skeletal muscle cell line and the T47-D breast carcinoma line were purchased from the ATCC. Fetal skeletal muscle cells (hSKM) were obtained from Clonetics.

For the TAT assay, H4-IIE cells were cultured in 96-well plates in DMEM/20% charcoal treated fetal bovine serum (FBS), 2 mM glutamine, 10 μU/ml penicillin and 1 mg/ml streptomycin sulfate overnight prior to compound evaluation. Compounds were dissolved in 100% DMSO and were added in medium to give a final DMSO concentration of 0.15%. Following an overnight incubation with the compounds, the medium was removed and the cells were lysed with 0.2 ml Promega lysis buffer by sonication for 1 min at room temperature. The lysis buffer was filtered using a Millipore multiscreen vacuum manifold and the filtrate collected as the source of tyrosine aminotransferase (TAT) for testing. TAT activity was measured as previously described, [2,25] and references within. For the antagonist experiments, full log scale (10^{-12} to 10^{-6}) titrations of the compounds were added in the presence of 15 nM Dex. The GS assay was performed as previously described in [23]. For the antagonist experiments, full log scale (10^{-12} to 10^{-6}) titrations of compounds were added in the presence of 10 nM dexamethasone for the rat L6 cells and 50 nM dexamethasone for the hSKM cells, respectively. The culture conditions for the L6 cells are also described in [23]. For the MMTV assay, A549 cells were seeded in 96-well plates (ca. 30,000 cells/well) in complete media (2.5% normal FBS/7.5% Charcoal treated FBS in H12-K media, LIFE Technologies). On day 2, fresh complete media was added and the compounds were added at a final DMSO concentration of 0.25% and incubated overnight at 37 °C. For all the experiments, the compounds were diluted in full log scale from 10^{-6} to 10^{-11} in DMSO. On day 3, the cells were

washed in (Ca^{2+} and Mg^{2+} free) 1× PBS and lysed in 1× reporter lysis buffer according to the manufacturers instructions (Promega). To the cell lysate, 100 μl of luciferase assay reagent/well (Promega) was added with an automatic injector. The light produced in the reaction was read in a microplate luminometer (EG&G Wallac) following a 10 s integration time. For the antagonist experiments, the compounds were added at concentrations from 10^{-12} to 10^{-6} in the presence of 10 nM Dex. In the MMP-1 studies, A549 cells were cultured in 90% F12 media and 10% charcoal/dextran stripped fetal bovine serum (sFBS). On day 1, near-confluent cells were seeded into 96-well tissue culture plates (ca. 30,000 cells/well) in 90% F12/10% sFBS. On day 4, fresh media was added, containing 100 ng/ml phorbol 12-myristate 13-acetate (PMA) and the ligands at a final concentration of 0.05% DMSO. The ligands and Dex were titrated at full log scale concentrations, from 10^{-12} to 10^{-6}. For the antagonist experiments the ligands were titrated at the same concentrations in the presence of 10 nM Dex. Following a 24-h incubation, the cell-conditioned media was harvested for ELISA determination. The amount of matrix metalloproteinase-1 (MMP-1; collagenase-1) was determined by ELISA using kits from The Binding Site (San Diego, CA). The ELISAs were performed following the manufacturers instructions. The optical densities at 450 nm were read on a Spectramax 25,096-well plate photometer. The EC_{50}s and IC_{50}s were calculated with the GraphPad Prism 3.0 software package using a single binding site sigmoidal dose response model. The data reported is derived from the duplicate wells from three independent experiments.

3. Results

3.1. Discovery of high affinity NSGCAs

Using a GRα ligand binding displacement assay (Section 2), the Merck compound collection was screened and the interesting spirocyclic dihydropyridine derivative **1** (Table 1), was identified as a lead. Compound **1** displaced ³H-dexamethasone in this assay, with an IC_{50} of 10 nM (Table 1). Based on the high GRα ligand binding affinity of **1**, a series of analogs was synthesized in which modifications were made around the dihydropyridine ring.
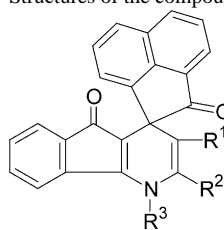
3.2. Synthesis of compounds 1–9

The dihydropyridine analogs **1–6** were synthesized by the Kats method, [14] employing a Hantzsch-type synthesis (Scheme 1, Section 2.2). Compounds **7–9** were prepared by N-alkylation of the dihydropyridine moiety of compound **2**.

3.3. GRα ligand binding of NSGCAs

The GRα ligand binding affinities of NSGCAs **1–9** are shown in Table 1. An increase in potency was achieved by

Table 1
Structures of the compounds and the IC$_{50}$s of the ligands to the GRα, MR and PR and AR

| Ligands				IC$_{50}$ in nM			
Compound	R^1	R^2	R^3	hGR	hPR	rMR	hAR
1	CONHPh	Me	H	10 ($\pm$1.52)	>1000	2300	>10000
2	CO$_2$Et	Me	H	1.4 ($\pm$0.6)	>1000	>10000	>10000
3	CO$_2$Bn	Me	H	2.1 ($\pm$0.7)	>1000	>10000	>10000
4	CONHBn	Me	H	97 ($\pm$42)	>1000	>10000	NA
5	CONEt$_2$	Me	H	430 ($\pm$199)	>1000	>10000	NA
6	CO$_2$Et	Ph	H	149 ($\pm$205)	>1000	>10000	NA
7	CO$_2$Et	Me	Me	1417 ($\pm$503)	>1000	>10000	NA
8	CO$_2$Et	Me	Bn	>5100	>1000	>20000	NA
9	CO$_2$Et	Me	CH$_2$OEt	3815 ($\pm$1185)	>1000	>10000	NA

The IC$_{50}$s were calculated as described in Section 2. The values reported are means of duplicate assay wells and are representative of three different experiments.

replacing the phenyl amide of **1** with an ethyl or benzyl ester giving **2** (IC$_{50}$ = 1.4 nM) and **3** (IC$_{50}$ = 2.1 nM) respectively. Other modifications of the phenyl amide of **1** proved to be detrimental to activity. The benzyl amide **4** was 5-fold less potent binder than **1** and 25-fold less active than the corresponding benzyl ester **3**. Replacement of the phenyl amide of **1** with a diethyl amide (compound **5**) resulted in a 20-fold loss of elative binding affinity (IC$_{50}$ = 231 nM). Introduction of a bulky phenyl substituent at the 2-position of the dihydropyridine ring (compound **6**) led to a drastic loss of activity (>100-fold) relative to the corresponding methyl analog **2**. In addition, the free N–H of **1** appeared to be necessary for

good activity, since the *N*-alkyl analogs **7**–**9** were very weak binders.

3.4. Selectivity of NSGCAs

Specificity for GRα was established in ligand binding assays with the PR, MR and AR (Section 2). As shown in Table 1, all the compounds tested lacked cross-reactivity with these highly related nuclear receptors. Notably, compounds **1**–**3**, have >100-fold selectivity for GRα, (Table 1). These compounds, which will be referred to as: NSGCAs **1**–**3**, were selected for further study.
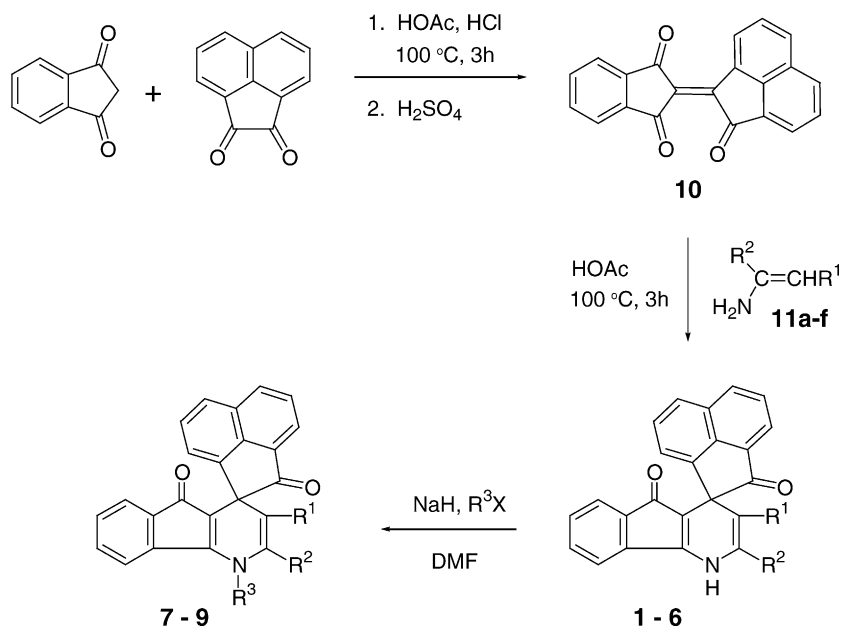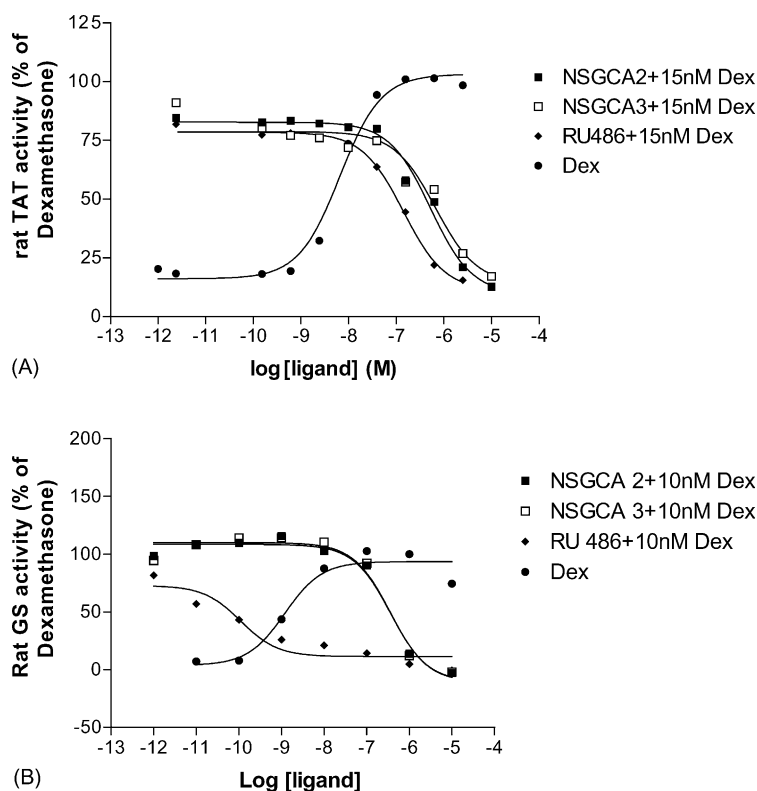

Scheme 1. Synthesis of compounds **1**–**9**.

Fig. 1. (A) NSGCAs **2** and **3** antagonize the Dex-dependent induction of rat TAT enzyme. The ability of NSGCA **2** (■), NSGCA **3** (□) and RU486 (♦) to antagonize the induction of the rat TAT enzyme in the presence of 15 nM Dex was tested. The induction of the rat TAT gene by the control compound, Dex is illustrated by (●). (B) NSGCAs **2** and **3** antagonize the dexamethasone-dependent induction of rat GS enzyme. NSGCA **2** (■), NSGCA **3** (□) and RU486 (♦) were tested as antagonists in the presence of 10 nM Dex in the rat GS assay. The control compounds, Dex (●) and RU486 (♦) were assayed in parallel to normalize the agonist and antagonist activity of the NSGCAs, respectively as indicated in Table 3. Data are means of duplicate assay wells from three independent experiments.

3.5. The NSGCAs are full antagonists of GC mediated transactivation in rodent cell lines

Although a large number of compounds bind to GRα, very few nonsteroidals have functional activity in cells. The ability of NSGCA ligands **1**–**3**, to induce biological responses was assessed by cell-based GRα transactivation assays using known GC responsive marker genes for glucose and glutamine metabolism. The tyrosine aminotransferase (TAT) enzyme [11] is a well characterized gluconeogenic gene known to be induced by GCs in vitro and in vivo. Therefore, TAT represents a useful marker gene to benchmark the analogs' effects on this gluconeogenic enzyme, TAT [11]. The effects on TAT activity were measured as described in the Section 2 in an established cell model of GC action, the rat liver cell line, H4IIE. In this cell line, the synthetic steroid Dex has been shown to robustly stimulate the transcription of this gene. Indeed, we show that Dex induces the TAT enzyme with an $EC_{50} = 2$ nM (Fig. 1A, Table 3). In the same assay, all the NSGCAs were virtually inactive as agonists of the TAT enzyme, with $EC_{50}s > 10,000$ nM and efficacy values of 2.5–4.0% relative to Dex (Table 2). However, when tested as antagonists in the presence of 15 nM Dex, (Fig. 1A, Table 3) NSGCAs **1**–**3** fully antagonized the Dex-dependent induc-

tion of TAT enzyme activity, with $IC_{50}s$ of 3 μM, 406 and 635 nM, respectively (Table 3, Fig. 1A). For the antagonist experiments, the efficacy of the NSGCAs as antagonists in the TAT assay and all the subsequent antagonist experiments was normalized to the efficacy of a well characterized GRα/PR antagonist compound, RU486. Thus the efficacy of RU486 at 10 μM was defined as100% (Tables 2–5).

Interestingly, RU486 was both a weak partial agonist and a full potent antagonist in the TAT assay, with an ag-

Table 2

Whole cell GRα ligand binding studies of NSGCAs **1**–**3** in rodent and human cell lines

Ligands	IC_{50} (in nM)			
	H4 cells	L6 cells	hSKM cells	MMTV-luc-A549 cell line
NSGCA **1**	688 ± 142	NA	NA	NA
NSGCA **2**	159 ± 28	124 ± 26	290 ± 80	237 ± 65
NSGCA **3**	281 ± 46	194 ± 47	270 ± 47	130 ± 35
Dex	5 ± 4	8.7 ± 2	9.4 ± 3	12 ± 6

For the competition experiments, 10 nM [1,2,4,6,7-³H]-Dex was utilized for all the cell lines tested. The $IC_{50}s$ were calculated as described in Section 2. The values reported are means of duplicate assay wells and are representative of three different experiments.

Table 3

Comparison of the NSGCAs agonist and antagonist activities in the rat TAT and GS GR transactivation experiments

Ligands	Agonist mode		Antagonist mode	
	EC_{50} (nM)	Percent max relative to Dex (Dex = 100%)	IC_{50} (nM)	Percent max relative to RU486 (RU486 = 100%)
Agonist and antagonist effects of NSGCAs in the rat TAT assay				
NSGCA **1**	>10000	4	3055 ± 916	97
NSGCA **2**	>10000	3	406 ± 16	90
NSGCA **3**	>10000	3	636 ± 116	96
Dex	5.2 (±0.32)	100		
RU486	39 (±6)	9	20 ± 2.1	100
Agonist and antagonist effects of NSGCAs in the rat GS assay				
NSGCA **1**	>10000	4	ND	ND
NSGCA **2**	>10000	2	306 ± 16	174
NSGCA **3**	>10000	3	413 ± 52	177
Dex	2.4 (±1.2)	100		
RU486	>10000	9	0.1 ± 0.04	100

The antagonist studies were performed in the presence of 15 nM Dex for the TAT gene and 10 nM for the GS gene. The EC_{50} and IC_{50} values were determined using a single binding site sigmoidal dose response model (Section 2). The agonist activity of the analogs is reported as a percent of the maximal transactivation activity of Dex, where the maximal activity of Dex at 10 uM is normalized to 100%. Similarly, the antagonist activity of the NSGCAs is reported as a percent of the maximal antagonist activity of RU486, assuming that the antagonist activity of RU486 is normalized to 100%. The values reported are means of duplicate assay wells and are representative of three different experiments.

Table 4

Effect of the NSGCAs on GR mediated transactivation of the MMTV-LTR luciferase and human GS promoters

Ligands	MMTV-luciferase		Human GS assay	
	IC_{50} (nM)	Percent max relative to Dex (RU486 = 100%)	IC_{50} (nM)	Percent max relative to RU486 (RU486 = 100%)
NSGCA **1**	ND	ND	ND	ND
NSGCA **2**	361 ± 30	140	1100 ± 92	92
NSGCA **3**	210 ± 22	132	659 ± 52	82
RU486	4 ± 2.4	100	6 ± 3.6	100

The antagonist experiments were performed in the presence of 10 nM Dex for the MMTV-LTR-luciferase promoter and 50 nM Dex for the human GS promoter. The IC_{50} values were determined using a single binding site sigmoidal dose response model (Section 2). The antagonist activity of the NSGCAs is reported as a percent of the maximal antagonist activity of RU486, where the antagonist activity of RU486 is normalized to 100%. The values reported are means of duplicate assay wells and are representative of three different experiments.

onist $EC_{50} = 39$ nM/10% maximal activity and an antagonist $IC_{50} = 20$ nM (Fig. 1A, Table 3). In contrast, NSGCAs **2** and **3** were full antagonists, with similar efficacy values as the reference antagonist, RU486 (Table 3).

Glutamine synthetase, (GS) is another GC-responsive enzyme that is known to be induced by GCs during catabolic states. The induction of GS has correlated with increases in protein turnover and gluconeogenesis. Therefore GS represents a useful marker to evaluate the effects of the NSGCAs on these biological processes. One cell model where the Dex dependent GS induction has been demonstrated, is the rat skeletal muscle cell line, L6 [18]. To follow the induction of

Table 5

Effect of the NSGCAs on GR mediated transrepression of the MMP-1 promoter

Ligands	Agonist mode		Antagonist mode	
	EC_{50} (nM)	Percent max relative to Dex (Dex = 100%)	IC_{50} (nM)	Percent max relative to RU486 (RU486 = 100%)
NSGCA **1**	ND	ND	ND	ND
NSGCA **2**	>10000	0	>10000	∼40
NSGCA **3**	>10000	0	>10000	∼50
Dex	3 ± 2.3	100		
RU486	0.3 ± 0.5	28	261 ± 36	100

For the agonist experiments, the agonist activity of the analogs is reported as a percent of the maximal transactivation activity of Dex (normalized to 100%). The analogs were also tested as antagonists in the presence of 10 nM dexamethasone as described in Section 2. The antagonist activity of the NSGCAs is reported as a percent of the maximal antagonist activity of RU486, where the antagonist activity of RU486 is normalized to 100%. The values reported are means of duplicate assay wells and are representative of three different experiments.

GS activity in L6 cells, a colorimetric assay [23] that measures the GS catalyzed γ-glutamyltransferase reaction was performed as described in Section 2. In this assay, Dex was a potent agonist, with an EC_{50} of 2.4 nM (Table 3). Consistent with the rat TAT assay, NSGCAs **2** and **3** completely abrogated the induction of GS by 10 nM Dex, with IC_{50s} of 306 and 413 nM, respectively. (Fig. 1B, Table 3) NSGCA **1** was excluded from this assay and the subsequent experiments due to its poor antagonist potency in the TAT assay (Table 3) and in the whole cell ligand binding assay (Table 2).

3.6. Whole cell ligand binding activity of NSGCAs

In the TAT GRα transactivation assay, NSGCAs **1**–**3** antagonized the Dex-dependent induction of this enzyme with different potencies. Therefore, the cell permeability properties of these ligands were evaluated by whole cell ligand binding analysis. In brief, the ability of NSGCAs to displace ^{3}H-Dex (10 nM) was tested in whole cells as described in Section 2. In this assay, NSGCA **1** bound GRα poorly in the H4 cell line, with an $IC_{50} = 700$ nM. Most likely, the lower antagonist potency of NSGCA **1** in the TAT assay can be explained in part by its lower potency in the whole cell ligand binding assay (Table 2). Moreover, the higher antagonist potency of NSGCAs **2** and **3** in the cell based assays is in good agreement with their potencies in the whole cell ligand binding studies (Table 2).

3.7. The NSGCAs are full antagonists in the GS and MMTV-luciferase assays in human cells

Given the nM antagonist potency of NSGCAs **2** and **3** in the rodent studies, we were interested in determining if these findings extended to human cells. Here primary human skeletal muscle cells (hSKM) were utilized to measure the ability of the NSGCAs to antagonize GC dependent induction of the GS gene. The GS assay was performed as described in Section 2. Similar to the rat GS assay, Dex was a potent inducer of human GS with EC_{50} of 8 nM (Table 4). Likewise, NSGCAs **2** and **3** completely antagonized Dex (50 nM) induced GS activity in primary hSKM cells with IC_{50s} of 1100 and 659 nM, respectively (Table 4, Fig. 2A).

The MMTV promoter is another classical GC-responsive gene, known to be transcriptionally regulated by GCs through a GRE-dependent mechanism and has been the subject of numerous studies on GC action. This model system was employed here as a direct comparator of the compounds' effects on a reporter based GRα regulated promoter (MMTV-LTR) to an endogenous GC-regulated gene, GS, and for subsequent studies where the antagonist effects of these ligands on GRα mediated transrepression and transactivation were measured in the same cell. For these studies, a stable cell line (MMTV-luc-A549) was made containing the MMTV-LTR luciferase reporter in the human lung epithelial cell line A549 (Section 2). In the MMTV-luc-A549 cell line, Dex also gave a strong induction of the MMTV-luc reporter with an EC_{50} of 2 nM.
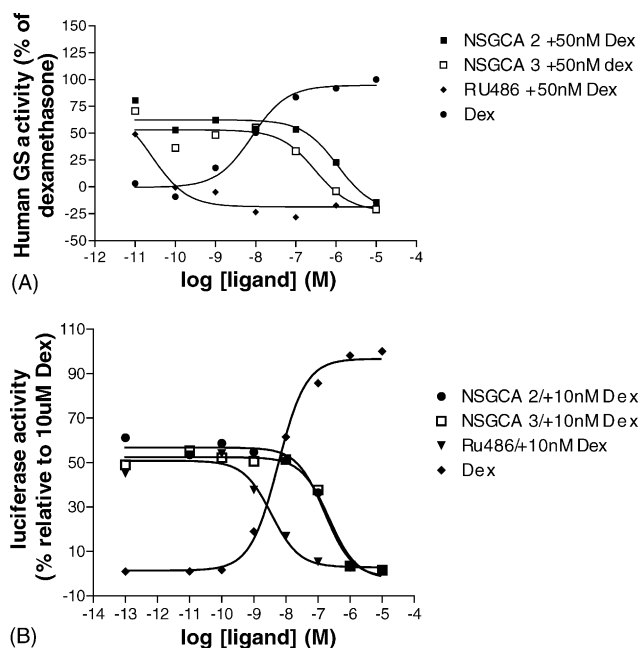

Fig. 2. (A) The NSGCAs are full antagonists in the hSKM GS GRα transactivation assay. NSGCA **2** (■), NSGCA **3** (□) and RU486 (♦) were tested in the presence of 50 nM Dex in the hSKM GS GRα transactivation assay. (B) Antagonist activity of NSGCA **2** and **3** in the human transactivation MMTV-luciferase reporter assay in the stable cell line A549-MMTV-luc. NSGCA **2** (■), NSGCA **3** (□) and RU486 (♦) were tested as antagonists in the presence of 10 nM Dex, as described in Section 2. The control compounds, Dex (●) and RU486 (♦) were assayed in parallel to normalize the agonist and antagonist activity of the NSGCAs, respectively as indicated in Table 4. Data are means of duplicate assay wells from three independent experiments.

Having established the MMTV-luciferase assay in the A549 cell line, we tested the NSGCAs as antagonists. In this assay, NSGCAs **2** and **3** were potent antagonists with IC_{50s} of 360 and 210 nM (Table 4, Fig. 2B). Compared to RU486, compounds **2** and **3** had similar fold differences in potency as the human GS studies (Table 4, Fig. 2B).

3.8. The NSGCAs are weak antagonists of the Dex-dependent transrepression of the proinflammatory enzyme, MMP-1

MMP-1 is a proinflammatory enzyme that is elevated in a variety of inflammatory conditions; including rheumatoid arthritis [4]. Importantly, GCs are known to counteract this inflammatory condition in large part by antagonizing the expression of proinflammatory genes such as MMP-1 [3]. Therefore, we evaluated the antagonist effects of the NSGCAs on the endogenous anti-inflammatory activity of GRα by measuring secreted protein levels of MMP-1. Interestingly, NSGCAs **2** and **3** were both poor agonists and weak antagonists of GRα mediated transrepression, with EC_{50s} and $IC_{50s} > 10,000$ nM (Table 5, Fig. 3) despite good whole cell GRα ligand binding activity in this cell line. By contrast, RU486 was a mixed partial agonist/full an-
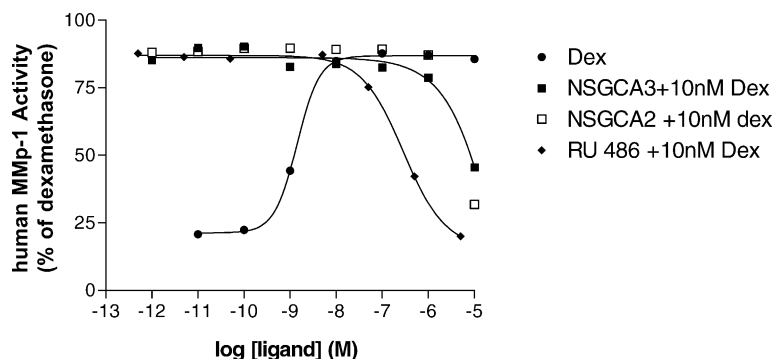
Fig. 3. Antagonist activity of NSGCAs **2** and **3** in the human MMP-1 GRα transrepression assay in the A549 cell line. NSGCA **2** (■) NSGCA **3** (□) and RU486 (♦) were tested as antagonists in the presence of 10 nM Dex, as described in Section 2. The control compound, Dex (●) and RU486 (♦) were assayed in parallel to normalize the agonist and antagonist activity of the NSGCAs, respectively as indicated in Table 5. Data are means of duplicate assay wells from three independent experiments.

tagonist of GC-dependent transrepression of the MMP-1 promoter; with an EC_{50} of 0.3 nM/28% maximal activity (Table 5) as a partial agonist and an $IC_{50} = 260$ nM as a full antagonist.

4. Discussion

In this study, we characterized novel GRα selective, small molecule NSGCAs by ligand binding and cell based functional assays. The ligand binding experiments, demonstrated that the free N–H of NSGCA **1** appears to be necessary for good activity, since the *N*-alkyl analogs **7**–**9** were very weak binders. In addition, replacement of the phenyl amide in NSGCA **1** with an ethyl or benzyl ester as in NSGCAs **2** and **3**, led to an increase in GRα ligand binding potency. From the nine spirocyclic dihydropyridine derivatives, NSGCAs **1**–**3** are the most potent ligands (Table 1). Notably, these NSGCAs have excellent GRα ligand binding affinity, with poor PR, AR and MR ligand binding activity. This finding is noteworthy considering the more than 50% homology between the ligand binding domains (LBD) of the GRα, AR, PR and MR [6,10,26].

In functional assays designed to measure GC mediated effects on endogenous marker genes of glucose and glutamine metabolism; we showed that NSGCAs **2** and **3**, are full antagonists of the GC-dependent induction of the endogenous activity of the TAT and GS enzymes. Importantly, this the first demonstration of functional antagonists of an endogenous metabolic marker gene of protein turnover, GS, in a recognized cell model of GC action, the L6 skeletal muscle cell line.

Of the three NSGCAs with functional activity in the TAT experiments, NSGCAs **2** and **3** had significantly higher antagonist potencies compared to the phenyl carboxamide derivative, NSGCA **1** (Table 3). One possibility for the lower antagonist potency of NSGCA **1** may be due to low cell permeability and or lower whole cell GRα ligand binding activity. The results of the whole cell GRα ligand binding studies in the

H4IIE and L6 cell lines are consistent with this explanation (Table 2).

In both the rat TAT and GS studies (Table 3) NSGCAs **2** and **3** had equivalent percent antagonist efficacy values as the reference compound, RU486. However, the NSGCAs antagonized Dex induction of the TAT and GS enzyme with different potencies relative to RU486. One possibility is that the NSGCAs differ in their intrinsic binding properties between the two cell types, the H4 and L6 cells. However, the whole cell binding studies strongly excludes this explanation, as the compounds have equivalent whole cell binding IC_{50}s in both cell types. More likely, the differences in the relative antagonist potency of the compounds at the rodent TAT and GS enzyme may be due in part to the higher potency of RU486 as an antagonist in the GS assay ($IC_{50} = 0.1$ nM, Table 3, Fig. 1B) compared to TAT assay ($IC_{50} = 20$ nM, Table 2, Fig. 1A). Although, these studies do not unequivocally delineate the mechanisms involved in the greater antagonist potency of RU486 in the GS studies, our findings do suggest a model whereby the conformation of the GR-RU486 complex at the GS promoter may be intrinsically different compared to the TAT promoter [2]. Consistent with this tenet we show that RU486 behaves as a partial agonist/antagonist in the TAT assay (Table 2, Fig. 1A and B), whereas it behaves as a pure antagonist at the GS promoter (Table 3). This mixed partial agonist/antagonist activity of RU486 in some cell and promoter contexts is well documented in the literature; thus this model is a plausible explanation for our observations with RU486 and the antagonist potency of the NSGCAs relative to RU486 in the rodent GS and TAT assays, respectively. However, unequivocal proof for this model warrants additional studies.

Collectively, the rodent TAT and GS studies suggest that the NSGCAs behave as pure antagonists at both the TAT and GS promoters; whereas RU486 may be a mixed partial agonist/antagonist at the TAT promoter and a pure antagonist at the GS promoter.

Having established the functional activity of these compounds in rodent cell models of GC action we then turned

our attention to characterizing them in human cells. Here, primary human skeletal muscle cells were utlized to monitor the effects of the NSGCAS on a marker gene for protein turnover, GS. In line with the rat GS studies, these ligands were full antagonists of Dex mediated induction of the GS enzyme with similar efficacy as RU486. Importantly, NSGCA **3** was a sub-micromolar antagonist with an $IC_{50} = 659$ nM (Table 4). To our knowledge these findings are novel and may have potential implications both at the research and drug discovery level. GS levels have been shown to be elevated in catabolic states, including muscle wasting; thus, a GR antagonist may be a viable alternative therapy for the treatment of this devastating disease.

The MMTV-LTR is a prototypical GRα regulated promoter that has been extensively cited in the literature and thus was used here in part, as a comparator for benchmarking the results with the endogenous GRα responsive promoters tested here. Consistent with the human GS transactivation studies, the NSGCAs antagonized the Dex-dependent induction of the MMTV-LTR luc reporter, with similar potency and efficacy (Table 4, Fig. 3A and B).

The potential utility of GR antagonists in the clinic is strongly dependent on a good therapeutic ratio. One potential side effect of GR antagonists would be to interfere with the endogenous anti-inflammatory activity of the GR. To address this potential liability of the NSGCAs, the expression levels of the proinflammatory enzyme, MMP1 were measured in the presence of Dex in the MMTV-luciferase A549 stable cell line. This cell model was chosen in order to simultaneously measure the effects of these ligands on both Dex mediated GR transactivation and transrepression, in the same cell line. Thus, offering the advantage of excluding cell type effects on the NSGCAs' potency. Importantly, the NSGCAs were inactive as agonists and weak antagonists of Dex mediated repression of the MMP-1 gene. Indeed, the dose response of the NSGCAs **2** and **3** as antagonists of the MMP-1 gene ($IC_{50} > 10,000$), was significantly right-shifted compared to their antagonist activity at the MMTV-luciferase reporter ($IC_{50} = 160$–210 nM). (Fig. 3, Table 5) Thus the later is consistent with the notion that the NSGCAs would not have minimal effects on the endogenous anti-inflammatory activity of the GRα, in this cell line. By contrast, RU486 was a mixed partial agonist/antagonist with an $EC_{50} = 0.3$ nM/30% max and an $IC_{50} = 260$ nM, respectively. Although, at first glance the results with RU486 in the GRα transrepression studies seemed unexpected, it appears that similar findings have been obtained with other cytokine promoters in the A549 cell line. Namely, RU486 was found to be a potent partial agonist of the cytokine granulocyte-macrophage colony stimulating factor (GM-CSF) with an $EC_{50} = 0.7$ nM/50% maximal efficacy [13]. Likewise, in GR transrepression studies in the osteosarcoma cell line, MG63, with concentrations as high as 100 nM RU486 only partially antagonized the Dex mediated repression of the cytokine IL-6 promoter.

The poor agonist/antagonist activity of NSGCAs **2** and **3** in the MMP-1 assay is not due to a lack of cell permeability because as mentioned earlier these compounds were potent antagonists of the Dex dependent induction of the MMTV-LTR luc reporter in the same cell line. Furthermore, the potencies of NSGCAs **2** and **3** in the whole cell GR ligand binding studies, in several cell types, including the A549 cell line where the MMP-1 gene was tested, strongly exclude this possibility (Table 1). One potential mechanism for the their lack of agonist activity in the MMP-1 assay may be due to their inability to recruit the appropriate cofactors that may be needed for maximal GRα mediated repression of the MMP-1 promoter. In this regard, the recent chromatin immunoprecipitation (CHIP) studies with the GM-CSF promoter in the presence of Dex or RU486 in the A549 cell line lend support to this notion [13]. In these studies, it was shown that complete repression of the GM-CSF gene by Dex, required abrogating p65-associated histone acetyl transferase (HAT) activity and the recruitment of Histone Deacetylase 2 (HDAC 2), to this promoter. Importantly, in parallel CHIP experiments with RU486, it was demonstrated that while RU486 was able to attenuate p65-associated HAT activity it did not recruit HDAC2 to the GM-CSF promoter. Finally, consistent with the CHIP studies, the GM-CSF ELISA studies that were cited earlier showed that RU486 inhibited the secretion of GM-CSF with 50% the efficacy of Dex. Taken together, the later provides a plausible explanation for our observations with RU486 and the NSGCAs in the MMP-1 GRα transrepression studies. However, this work cannot exclude for the potential for additional and or alternative mechanisms to be involved in the mode of action of these ligands. Future studies will be required to further define the mechanism of action of these novel ligands.

5. Significance

The extensive literature on RU486 has strongly implicated GCs in the pathogenesis of insulin resistance [2,7–9,15,16]. GC excess due to hyperactivity of the hypothalamic–pituitary–adrenal (HPA) axis, or to increases in GRα sensitivity in peripheral tissues, or to altered cortisol metabolism have all been correlated with insulin resistance states [1]. Thus a GRα-selective antagonist may be a reasonable therapeutic agent for lowering plasma glucose levels in Type II diabetics. Here we have identified NSGCAs that completely antagonized the GC-dependent induction marker genes for glucose and glutamine metabolism: TAT and GS in vitro. Importantly, to our knowledge antagonists of the GS enzyme activity are novel and could have potential therapeutic applications for the treatment of muscle wasting. Moreover, with the NSGCAs significant right shift in potency as antagonists of Dex mediated transrepression of the MMP-1 promoter, it may afford these compounds an improved therapeutic ratio.

Finally, the recent disclosure by other members of the pharmaceutical industry of functional and selective GRs (sGRMs) provides additional evidence that novel NSGCAs can be obtained [20–22]. Hence, the NSGCAs described here, should stimulate further efforts to explore the potential for NSGCAs to lower plasma glucose levels and protein catabolism in vivo.

References

[1] R.C. Andrews, B.R. Walker, Glucocorticoids and insulin resistance: old hormones, new targets, Clin. Sci. (Colch) 96 (1999) 513–523.

[2] C.M. Bamberger, G.P. Chrousos, The glucocorticoid receptor and RU 486 in man, Ann. N. Y. Acad. Sci. 761 (1995) 296–310.

[3] C.M. Bamberger, H.M. Schulte, G.P. Chrousos, Molecular determinants of glucocorticoid receptor function and tissue sensitivity to glucocorticoids, Endocr. Rev. 17 (1996) 245–261.

[4] M. Bond, A.H. Baker, A.C. Newby, Nuclear factor kappaB activity is essential for matrix metalloproteinase-1 and -3 upregulation in rabbit dermal fibroblasts, Biochem. Biophys. Res. Commun. 264 (1999) 561–567.

[5] M.E.F. Braibante, H.S. Braibante, L. Missio, A. Andricopula, Synthesis and reactivity of β-amino α,β-unsaturated ketones and esters using K-10 montmorillonite, Synthesis (1994) 898–900.

[6] R.M. Evans, The steroid and thyroid hormone receptor superfamily, Science 240 (1988) 889–895.

[7] J.E. Friedman, Y. Sun, T. Ishizuka, C.J. Farrell, S.E. McCormack, L.M. Herron, P. Hakimi, P. Lechner, J.S. Yun, Phosphoenolpyruvate carboxykinase (GTP) gene transcription and hyperglycemia are regulated by glucocorticoids in genetically obese db/db transgenic mice, J. Biol. Chem. 272 (1997) 31475–31481.

[8] J.E. Friedman, J.S. Yun, Y.M. Patel, M.M. McGrane, R.W. Hanson, Glucocorticoids regulate the induction of phosphoenolpyruvate carboxykinase (GTP) gene transcription during diabetes, J. Biol. Chem. 268 (1993) 12952–12957.

[9] D.R. Garrel, R. Moussali, A. De Oliveira, D. Lesiege, F. Lariviere, RU 486 prevents the acute effects of cortisol on glucose and leucine metabolism, J. Clin. Endocrinol. Metab. 80 (1995) 379–385.

[10] V. Giguere, S.M. Hollenberg, M.G. Rosenfeld, R.M. Evans, Functional domains of the human glucocorticoid receptor, Cell 46 (1986) 645–652.

[11] D. Granner, S. Pilkis, The genes of hepatic glucose metabolism, J. Biol. Chem. 265 (1990) 10173–10176.

[12] P.O. Hasselgren, Glucocorticoids and muscle catabolism, Curr. Opin. Clin. Nutr. Metab. Care 2 (1999) 201–205.

[13] K. Ito, E. Jazrawi, B. Cosio, P.J. Barnes, I.M. Adcock, p65-activated histone acetyltransferase activity is repressed by glucocorticoids: mifepristone fails to recruit HDAC2 to the p65-HAT complex, J. Biol. Chem. 276 (2001) 30208–30215.

[14] A.M. Kats, G.D. Tirzit, G.Y. Dubur, Preparation of 8-(5-oxoindeno[3,2-b]-4-pyridyl)-1-naphthoic acids, Chem. Heterocyclic Compd. (USSR) 8 (1972) 188–189.

[15] H. Kodama, M. Fujita, I. Yamaguchi, Development of hyperglycaemia and insulin resistance in conscious genetically diabetic (C57BL/KsJ-db/db) mice, Diabetologia 37 (1994) 739–744.

[16] M. Kusunoki, G.J. Cooney, T. Hara, L.H. Storlien, Amelioration of high-fat feeding-induced insulin resistance in skeletal muscle with the antiglucocorticoid RU486, Diabetes 44 (1995) 718–720.

[17] A.H. Li, S. Moro, N. Melman, X. Ji, K.A. Jacobson, Structure–activity relationships and molecular modeling of 3,5-diacyl-2,4-diakylpyridine derivatives as selective A3 adenosine receptor antagonists, J. Med. Chem. 41 (1998) 3186–3201.

[18] S.R. Max, J.W. Thomas, C. Banner, L. Vitkovic, M. Konagaya, Y. Konagaya, Glucocorticoid receptor-mediated induction of glutamine synthetase in skeletal muscle cells in vitro, Endocrinology 120 (1987) 1179–1183.

[19] L. Mercier, E.B. Thompson, S.S. Simons Jr., Dissociation of steroid binding to receptors and steroid induction of biological activity in a glucocorticoid-responsive cell, Endocrinology 112 (1983) 601–609.

[20] J.N. Miner, C. Tyree, J. Hu, E. Berger, K. Marschke, M. Nakane, M.J. Coghlan, D. Clemm, B. Lane, J. Rosen, A nonsteroidal glucocorticoid receptor antagonist, Mol. Endocrinol. 17 (2003) 117–127.

[21] B. Morgan, Selective glucocorticoid receptor modulators, in: Proceedings of the Gordon Conference on Medicinal Chemistry, Colby Sawyer College, New London, NH, 2001.

[22] B.P. Morgan, A.G. Swick, D.M. Hargrove, J.A. LaFlamme, M.S. Moynihan, R.S. Carroll, K.A. Martin, E. Lee, D. Decosta, J. Bordner, Discovery of potent, nonsteroidal, and highly selective glucocorticoid receptor antagonists, J. Med. Chem. 45 (2002) 2417–2424.

[23] J.C. Santoro, G. Harris, A. Sitlani, Colorimetric detection of glutamine synthetase-catalyzed transferase activity in glucocorticoid-treated skeletal muscle cells, Anal. Biochem. 289 (2001) 18–25.

[24] G.Y. Vanag, L.S. Geita, The condensation of acenaphthenequinone with 1,3-indandione, J. Gen. Chem. USSR 26 (1956) 539–543.

[25] B.M. Vayssiere, S. Dupont, A. Choquart, F. Petit, T. Garcia, C. Marchandeau, H. Gronemeyer, M. Resche-Rigon, Synthetic glucocorticoids that dissociate transactivation and AP-1 transrepression exhibit antiinflammatory activity in vivo, Mol. Endocrinol. 11 (1997) 1245–1255.

[26] S.P. Williams, P.B. Sigler, Atomic structure of progesterone complexed with its receptor, Nature 393 (1998) 392–396.